

MODELLING OF LIQUEFACTION AND LATERAL SPREADING

S P Gopal Madabhushi, B Teymur, S K Haigh and A J Brennan
Department of Engineering, University of Cambridge, England

Abstract: In this paper we outline recent developments in dynamic centrifuge modelling at Cambridge University. The developments to the new Stored Angular Momentum (SAM) earthquake actuator are outlined. The importance of investigation and quantifying the boundary effects in centrifuge model containers is emphasised. The use of miniature CPT devices to quantify the boundary effects in the Equivalent Shear Beam (ESB) model containers is explained. Development of a new, large ESB model container to investigate liquefaction under high confining pressures is outlined. The use of the dynamic centrifuge testing capabilities to study problems on liquefaction induced lateral spreading, soil flow past piles and in understanding the efficacy of drains as liquefaction mitigation measures is presented. The results from the above testing will be discussed in the light of their contribution understanding the fundamental soil behaviour under earthquake loading as well as to improving design methods and guidelines.

1 Introduction

Recent earthquakes in Turkey, Greece, Taiwan and India have highlighted the need to understand the complex behaviour of civil engineering structures when subjected to powerful earthquake vibrations. The Bhuj earthquake of 26th January 2001 highlighted some of the complex problems associated with liquefaction of ground. For example let us consider a bridge site near the towns of Bhachau and Vondh during the Bhuj earthquake. At this site four bridges cross the river channel which has clearly liquefied with extensive sand boiling being observed next to the piers as seen in Fig.1. The four bridges had different types of superstructure, for example the new railroad bridge had plate girder spans while the old bridge was of arch construction (seen in Fig.1 behind the plate girder bridge). The ground motion at the site was approximately parallel to the longitudinal axis of the bridges.



Fig.1 Liquefied bridge site during Bhuj earthquake of 2001

Liquefaction of the foundations led to the rotation of the piers of the plate girder bridge as seen in Fig.2. On the other hand the arch bridge suffered loosening of the crown stones due to movement of the thrust blocks supported on the pier. Following the earthquake, resin was injected to fix the crown stones in place as seen in Fig.3. It appears that liquefaction of the foundation led to the different behaviour of these two bridges. The plate girder bridge has relatively low torsional stiffness and it was possible for the piers to suffer rotation about the

longitudinal axis of the bridge. The arch bridge, on the other hand, has a high torsional stiffness and the damage here was due to the movement of the piers along the longitudinal axis thereby allowing the loosening of the crown stones. It appears that the superstructure stiffness influences and determines the failure mode in which the bridge may suffer damage once the foundations have liquefied, Madabhushi et al (2001).



Fig.2 Piers of plate girder bridge suffered rotation



Fig.3 Crown stones of the arch opened up due to abutment movement

The Bachau-Vondh bridge site highlights the complexity of the behaviour of soil structure systems when the soil suffers liquefaction following earthquake loading. Modelling of the liquefaction of foundations and the superstructure is important to understand such problems.

Dynamic centrifuge modelling offers an opportunity to understand failure mechanisms such as those described above. In this paper we outline some of the facilities for earthquake modelling that were

recently developed at the Schofield Centre at Cambridge University. We emphasise the importance of understanding the stress state and the soil stiffness of the soil model at high gravity and of quantifying the boundary effects imposed on the model. We also illustrate the use of the facility to model the problems of liquefaction induced lateral spreading, soil flow past piles and the use of gravel drains to mitigate liquefaction. These investigations reveal how dynamic centrifuge modelling can help to clarify the underlying mechanisms at work and how the results from modelling can help geotechnical practice while dealing with earthquake problems.

2 Stored Angular Momentum (SAM) Earthquake Actuator

Earthquake modelling at Cambridge University started as early as late 1970's. Early earthquake actuators used were based on leaf springs followed by the famous 'Bumpy Road' actuator developed by Kutter (1982). The Bumpy road actuator was used extensively for a decade and a fundamental understanding of liquefaction was achieved through investigation of many boundary value problems. Since 1995 the Stored Angular Momentum (SAM) earthquake actuator, Madabhushi (1998), has superseded the Bumpy road actuator.



Fig.4 An overview of the Stored Angular Momentum (SAM) Earthquake Actuator



Fig.5 Self-contained swinging platform carries both the SAM actuator and the ESB soil model container

The SAM earthquake actuator is a mechanical device which stores the large amount of energy required for the model earthquake event in a set of flywheels. At the desired moment this energy is transferred to the soil model via a reciprocating rod and a fast acting clutch. When the clutch is closed through a high pressure system to start the earthquake, the clutch grabs the reciprocating rod and shakes with an amplitude of ± 2.5 mm. This is transferred to the soil model via a bell crank mechanism. The levering distance can be adjusted to vary the strength of the earthquake. The duration of the earthquake can be changed by determining the duration for which the clutch stays on. Earthquakes at different frequency tone bursts can be obtained by selecting the angular frequency of the flywheels. In Fig. 4 we present an overview of the SAM actuator.

Recent modifications to the SAM actuator were carried out to further enhance its capabilities and to improve the performance envelope. Early earthquakes using this device were non-symmetric as the clutch migrated downwards to an end stop once the centrifugal acceleration was applied. This meant that at the start of the earthquake the clutch body was hitting the end stop if it grabbed the reciprocating rod during its downward motion. This problem has been rectified by incorporating a pneumatic actuator that centralises the clutch prior to every earthquake. Logic controls automatically turn the air to the pneumatic actuator off once the earthquake is fired and the clutch starts to move with the reciprocating rod. Another improvement that was made to the SAM actuator was development of a self-contained swing. This meant that the model container and SAM actuator are mounted on one swing that can be easily loaded and unloaded from the 10m beam centrifuge. This development has greatly improved the operational efficiency at the Schofield Centre while conducting the dynamic centrifuge tests. Given that the 10m beam centrifuge is used every week through out the year, dynamic centrifuge tests can now be conducted with very little downtime of the facility while changing from 'static' centrifuge tests. In Fig.5 we present an overview of the self-contained swing along with the smaller of the two Equivalent Shear Beam (ESB) model containers. A new, large Equivalent Shear Beam (ESB) model container is also being developed. This will be explained in Sec. 4 of this paper.

The salient features of the SAM earthquake actuator are outlined below.

- 100 g operation
- Two model containers representing prototype dimensions at 100g of
56 m (L) \times 25 m (B) \times 22 m (H)
or 80 m (L) \times 25 m (B) \times 40 m (H)
- Earthquake Strength of Choice (up to 0.4 PGA)
- Earthquake Duration of Choice (from 0 s to 150 s)
- Earthquake Frequency of Choice (from 0.5 Hz to 5 Hz) and Swept Sine Wave Capability

Note: All parameters above are in prototype scale

3 Equivalent Shear Beam (ESB) Model Containers

The Equivalent Shear Beam (ESB) model container has flexible frictional end-walls designed to move together with the soil inside and to sustain the complementary shear force induced by

base shaking. It was designed to achieve the same deflection and natural frequency as an ideal prototype soil layer with thickness, $H=10\text{m}$, void ratio, $e=0.77$ ($I_D=50\%$) and unit weight, $\gamma=15\text{kN/m}^3$ under an earthquake of 30% at 50g. The dimensions of the ESB container are $560\text{mm}\times 250\text{mm}\times 223\text{mm}$ built with alternating rectangular layers of aluminium and rubber. Special features include inextensible friction sheets attached to each end-wall. These 0.5mm thin aluminium sheets were roughened by gluing sand onto them to transfer the shear stresses to the base of the container to overcome the overturning moment created in compression and extension (Zeng and Schofield, 1996).

A series of centrifuge tests involving loose and dense, dry and saturated models of homogeneous horizontal sand layers have been carried out with measurements being taken to quantify the effects of the boundaries on soil behaviour. Miniature CPT tests were conducted in flight, before and after earthquake loading to investigate boundary effects. Densification of sand near the end walls during dynamic loading may be impeded due to arching and shear transfer to the walls. The CPT was used for comparison of the results since only total penetration resistance was logged. This of course would consist of both shaft friction and end bearing components. Since penetration resistances at different locations and at different times (i.e. before and after earthquake loadings) were compared, it was felt that the shaft friction and end bearing components need not be measured separately (Teymur and Madabhushi, 2001). The miniature CPT device has a 6mm diameter rod fitted with a 60° conical tip with a load cell placed at the top of the rod to measure the total force applied.

In Fig. 6, the results of penetration tests on a saturated loose sand model with a relative density of $I_D=54\%$ before and after the earthquake are shown. The plots of centre and end

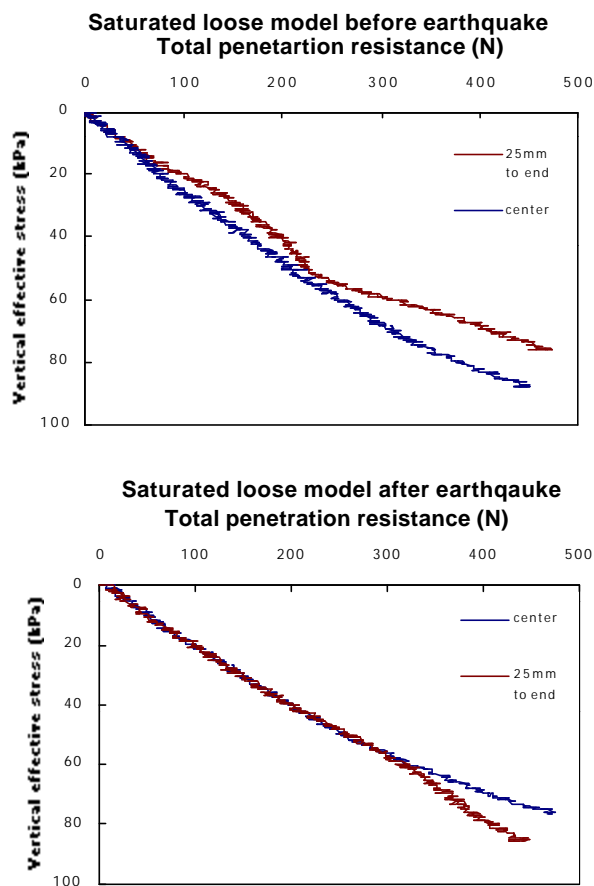


Fig.6. Penetration resistances before and after the earthquake in saturated sand model

resistances are similar up to 5m, but after this depth the pre-earthquake these values diverge. In the case of saturated models, the effective stress is much smaller, there by reducing the arching effect near the boundary during swing-up. Due to the lower effective stress the CPT resistance is more or less same throughout the saturated model especially at shallow depths as seen in Fig.6. An earthquake of magnitude 10% was applied and following that the CPTs were repeated. After the earthquake the difference between sites gets smaller up to 6m depth. Below this depth the resistance at the end and the centre starts to deviate. Up to this depth the soil layer became uniform as the arching effect observed before the earthquake has been destroyed. Below this depth the effect of shear stresses due to arching on penetration resistance is seen. (Teymur and Madabhushi, 2001). Results show the resistance at the centre to be more than the resistance at the end-walls. The reason for this behaviour may be that the soil layer does not have the same

settlement as the end wall during swing up and the rough boundary would be holding the sand up causing boundary effects to be observed.

The results from the above experiments show that there is a difference in the soil stiffness before and after the earthquake loading due to the presence of rough shear sheets placed at the end walls. The concept of shear sheets was developed with the view of generating complementary shear stresses at the boundaries in sympathy with the lateral shaking at the base, thereby avoiding any dynamic moment being generated about the centroid of the soil model, Madabhushi et al (1995). These sheets are clearly meant to work during the earthquake loading. The results from the current study show the effects of the complementary shear sheets prior to and after the earthquake loading. Clearly the rough sheets at the end walls are providing arching in the soil following earthquake loading, when the rest of the soil sample undergoes settlement. This research has shown that CPT tests produce consistent and reliable data to interpret the influence of the boundaries. The results suggest that the complementary shear sheets cause differences in the soil behaviour between the centre and the end-walls.

4 A New Equivalent Shear Beam Container

Recently, questions have been asked about liquefaction potential at depth. Can sufficient pore pressures be maintained, or even generated, to cause soil liquefaction problems in soil under high confining stress. Steedman (1999) discusses a recently initiated a program at US army Waterways Experiment Station in Vicksburg, MI of centrifuge testing of deep deposits. Initial findings indicate a possible development of higher mode shapes during shaking. Aside from this, treatment of the subject in the literature is scarce, possibly due to the requirement for field data and/or high-pressure modelling equipment. It is thought that centrifuge modelling can contribute decisively to the debate.



Fig.7 A view of the new large Equivalent Shear Beam (ESB) model container

The new container seen in Fig.7 consists of 10 rings, each 38.1mm by 63.5mm box section. Internal dimensions are 653mm \times 253mm \times 427mm high, so soil depths of up to 40m may be modelled. Intervening rubber layers are 4mm thick in the lowest 4 rings where shear stress is highest, and 6mm thick in the topmost 5 where lower shear stresses generate smaller deflections per unit thickness. This is the first time this idea has been incorporated in an ESB container. This ESB model container also incorporates safety features such as a half-inch studding going through the end walls with sufficient clearance around it to allow for free vibration

of end walls during shaking. The studding will only be brought into play if the glue joints fail during shaking and holds all the rings together under such circumstances until the centrifuge can be safely stopped. In extending the ESB concept to deeper containers, one needs to consider the lateral deflection of the long sidewalls under significant lateral pressures. Should these bulge too much, the K_0 condition in the model does not match that intended in the

prototype. Use of box sections ensured maximum stiffness for minimum weight gain (Brennan & Madabhushi, 2002).

5 Liquefaction-induced Lateral Spreading

Liquefaction and lateral spreading of saturated, gently sloping, loose, fine sand deposits is a matter of concern during earthquakes. Investigation of the Niigata earthquake of 1964 revealed extensive lateral spreading with up to 10m of surface displacement being seen close to the Shinano river. The damage in this earthquake was extensively studied by Hamada (1992) who gives details of much of the damage caused. Ground movements of this magnitude obviously cause great damage to the structures founded upon them, more than any other form of liquefaction induced ground failure, (National Research Council (1985)). This damage can include movement of quay walls, axial buckling of bridge decks and railways spanning between spreading slopes and bending failure of piles passing through laterally spreading liquefiable layers.

Lateral spreading especially occurs close to free boundaries such as rivers, the shore or quay walls, as here the water table is high and the boundary conditions favourable. A large volume of case study data is available on lateral spreading towards these free boundaries from previous earthquakes. Dynamic centrifuge modelling was carried out using sloping laminar boxes at RPI by Abdoun (1997), and finite element modelling at Cornell by Meyersohn (1994). Much of the data from field studies of the extent of lateral spreading is based on aerial photogrammetry or satellite imaging, comparing photographs from before and after the earthquake and measuring the movement of objects dragged with the lateral flow, such as manholes and some buildings, relative to certain fixed points. Unfortunately this technique can only give surface displacements for the soil.

Over the last three years, a series of centrifuge tests have been carried out at Cambridge to investigate the liquefaction-induced lateral spreading of gentle slopes. These centrifuge models consisted of beds of Fraction E silica sand with a D_{50} size of 0.15mm, air-pluviated to a relative density of approximately 40%, with slope angles of between three and twelve degrees. The models were saturated inflight with 50 cS silicone oil and were subjected to base shaking using the SAM earthquake actuator.

Many interesting results have been observed from this test series concerning the dynamic behaviour of liquefiable slopes, particularly the effects of dilation on the observed response. The ground displacement profile observed during one of the tests by means of coloured sand markers is shown in Fig.8. It can be seen that the peak displacement observed is not at the surface, but at a depth of approximately 1m (prototype scale). It is postulated that this is due to restraint from the end walls of the box, rather than being a true infinite slope phenomenon. This hence corresponds more closely to such field examples as lateral spreading towards a structure such as a quay wall, or towards a plane of symmetry such as a river centreline, rather than to free-field motion. The dynamic behaviour of the slope was studied using miniature instrumentation for the measurement of pore-pressures and accelerations throughout the slope. Analysis of these signals has revealed interesting details about the response of these slopes to earthquake loading. The accelerometer time-histories in Fig.9 show the measured base and surface accelerations in one of the models. It can be seen that whilst the base motion

is approximately constant from cycle to cycle, the surface response late in the earthquake shows alternate cycles having profoundly different behaviour.

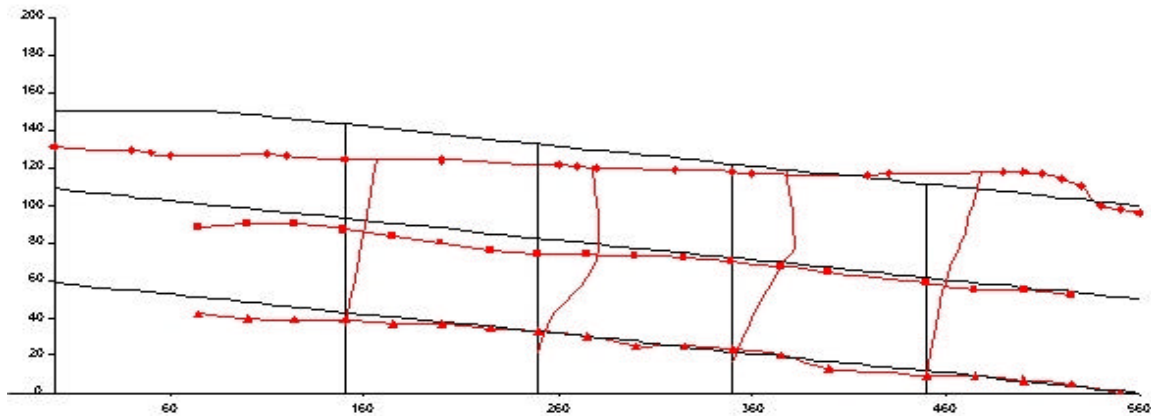


Fig.8 Slope displacements due to lateral spreading of the slope

This shows itself as an amplified frequency component at half of the fundamental earthquake frequency upon study of FFT's. Measurement of the phase lag of acceleration between base and surface of the models, as could be achieved from the time-histories shown in Fig.10, allows estimates of the shear wave velocity to be made at different times during the earthquake. From this data it can be shown that as the soil liquefies and softens, the shear wave velocity falls to such a point that the natural frequency of the soil column becomes approximately 25 Hz, half that of the earthquake excitation. It is thus postulated that the soil column is resonating at this natural frequency, hence giving the behaviour described above.

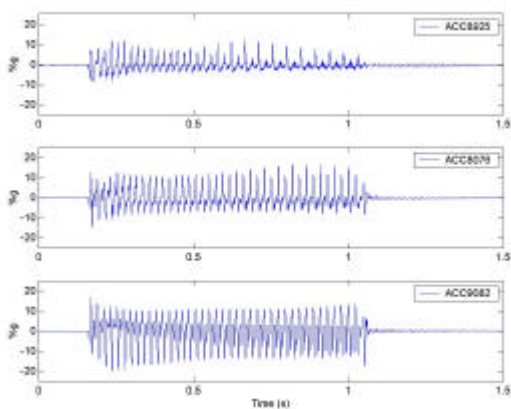


Figure 9 Acceleration time-histories

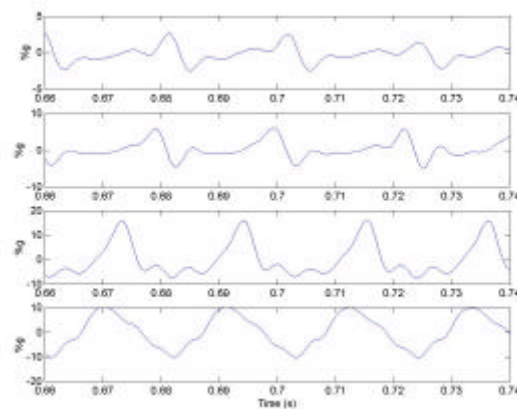


Figure 10 Upwards propagation of S-wave

It is also interesting to note the dilative response of the soil slope. All of the PPT's present in the model show significant dilative behaviour occurring with the generation of a "suction-spike" once per cycle. Examining the timing of these spikes with respect to depth illustrates that this suction pulse propagates vertically from the base of the model to the surface at the shear wave velocity. This behaviour is illustrated in Fig.11. It is postulated that this is due to the dynamic shear stress applied by the wave, superimposed on the initial static shear stress causing the soil stress path to cross the characteristic state threshold and hence the soil to dilate. This pore-pressure behaviour will cause a slip-stick motion of the soil down the slope, with velocity and displacement being accumulated while the base is accelerating upslope and then locking up on the other half-cycle when dilation occurs.

6 Piles in laterally spreading soils

Whilst the lateral spreading of slopes during earthquakes can be a major problem for geotechnical structures such as dams and embankments, as was seen from the massive lateral spreads observed at Navalakhi port during the 2001 Bhuj earthquake shown in Fig. 12, (EEFIT, 2001), further problems can be caused from the interaction of laterally spreading soils with foundations or pipelines passing through them. Damage due to this interaction has

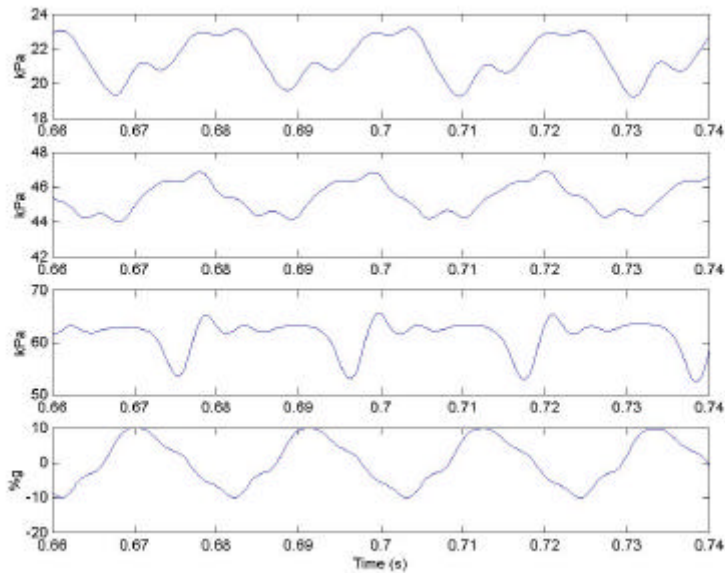


Figure 11 Upward propagation of suction spike



Figure 12 Lateral spreading at Navalakhi port.

laterally spreading slopes have on pile foundations passing through them. The model slopes contained flexible piles, instrumented with strain gauges to measure the induced bending moments. Pore pressures were also measured at locations close to the upslope and down slope faces of the piles.

been observed in many major earthquakes, including such collapses as the Showa bridge in the 1964 Niigata earthquake, as illustrated in Fig. 13. It can be seen that the combination of the forces induced by the laterally spreading soil and inertial and axial forces from the superstructure have caused failure of the piles, resulting in the bridge decks being toppled.

Following on from the work described in Sec.5, a series of centrifuge experiments has been carried out to investigate the effects that the



Figure 13 Collapse of the Showa bridge in the 1964 Niigata earthquake (after Hamada 1992).

Whilst the bending moment data shown in Fig.14 shows that, as expected, significant bending moments were induced in the piles due to the influence of the laterally spreading soils, study of the pore-pressures measured close to the pile faces shows more clearly the mechanism of the interaction occurring.

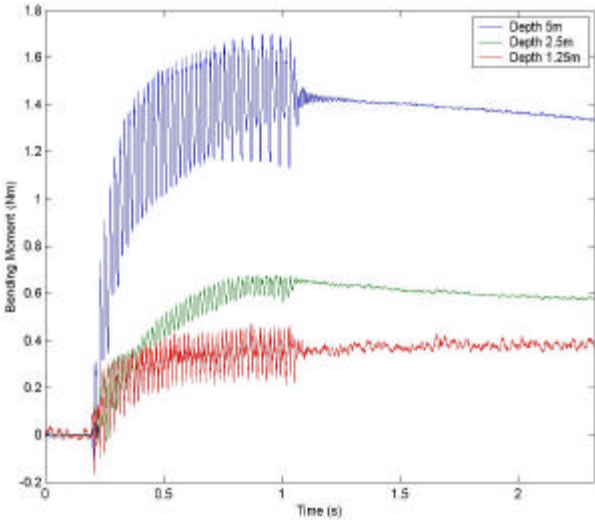


Fig. 14 Measured pile bending moments

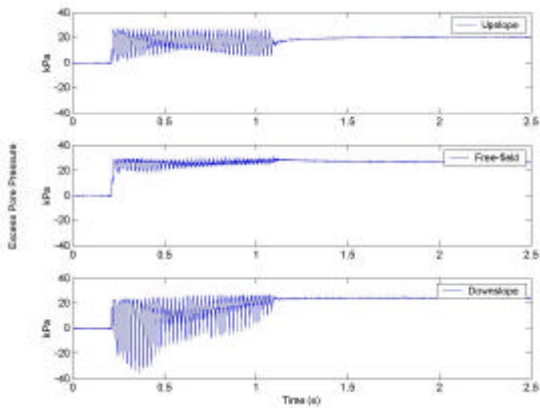


Fig. 15 Near pile pore-pressure time-histories

Figure 15 shows the pore-pressures measured close to the upslope and downslope faces of the pile. It can be seen that both records show significant suction spikes once per cycle, with these being more significant downslope of the pile. This behaviour can be explained by considering the stress path that soil elements close to the pile experience from within a characteristic state framework, (Luong & Sidaner, 1981). The total and effective stress paths for these elements are plotted in Fig.16. It can be seen that soil elements immediately upslope of the pile experience an increasing horizontal stress due to flow, whereas those down slope of the pile experience horizontal stress relaxation. Because the initial value

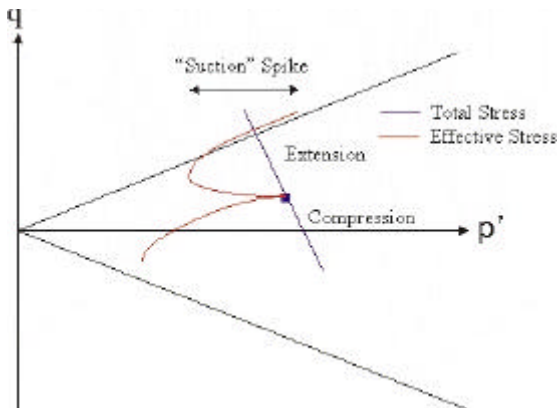


Fig. 16 Soil element stress-paths

of K_0 is less than unity, being approximately 0.5, this results in less stress increment being needed to reach the characteristic state threshold downslope of the pile than upslope and hence, under equal stress increments, more dilative behaviour being observed down slope of the pile.

Measuring the pore-pressure difference between the front and back faces of the piles reveals a peak difference of approximately 60 kPa at 3.5m depth. The current Japanese highway bridges design code, (JRA 1996), specifies that for piles passing through sloping liquefiable soils, horizontal loads should be assumed as 30% of total overburden stress, corresponding to approximately 20kPa at 3.5m, one third of the measured peak transient pore-pressure difference. This does however correspond more closely to the post-earthquake residual pressure difference of 20kPa. Efforts have also been made to measure the contact stresses exerted on the faces of both rigid and flexible piles, but these are still at a preliminary stage. From these results it is also possible to compare the applied loads and induced bending

moments directly for a particular test, the relationship not being given by a double integral owing to the dynamic behaviour of the pile, the pile not being in static equilibrium during the earthquake and measured moments hence being a function of accumulated strains, rather than imposed stresses.

Comparison was also made between the performance of piles of square and circular section. It as noted from the displacement of coloured sand markers that the zone of influence of the circular pile was of greater extent perpendicular to the flow direction, but of lesser extent parallel to the flow than that of the square pile. The soil exhibited flow separation down the sides of the square pile, with a grabben forming upslope of the pile and a trench down slope, whereas the circular pile caused all the soil to deviate around the obstruction.

7 Liquefaction Remediation by Vertical Drains

Vertical drains operate by providing preferential drainage paths which enable accumulating pore pressures to dissipate ideally before the surrounding soil reaches a state of initial liquefaction. Another method of achieving this result is the vibro-replacement stone column which is primarily a soil densification treatment with the added benefit of drainage. Faced with this new competition, pure drainage systems appear to be going out of fashion. This could be due to the questionable field performance seen, where some treated areas have still settled unsatisfactorily, as reviewed by Mitchell et al (1995). It is probable that this results from outdated design methods, maintained by industrial inertia and limited understanding of the problem.

Seed & Booker (1977) initially solved the dissipation equation computationally under the boundary conditions of a cylinder containing a centrally located drain and zero horizontal hydraulic gradient at the outer boundary, a “unit cell”. The problem is assumed as axi-symmetric and vertical dissipation is ignored. Their numerical method involved several assumptions that have since been shown to be overly simplistic. Research following this, as reviewed by Boulanger et al (1995), demonstrated the fallacy of ignoring pore pressures in the drain and often provided new charts to follow. These more recent studies have, however, often remained focused on the unit cell. In the chart based approach no consideration is given to the drain radius a in terms of confirming drain capacity to be adequate. There is also no dependence on any depth coordinate, neither soil layer depth nor thickness.

If extremely large areas were covered in equally spaced drains, each would only affect the local area as shown in Fig.17. Each would, in effect, have its own drainage basin and watershed, and would be concerned only with fluid within this “unit cell”. Flow is not permitted across the boundary. In this large-number-of-drains limit, the unit cell theory is sound. It also represents an ultimate limit, the optimal situation where the drain is responsible for the minimum possible amount of pore-fluid. Conversely, if there were only one drain in this extremely large area, it would be unlikely to prevent liquefaction anywhere. As soon as fluid were removed from its vicinity, more comes from further away to replace it and maintains high pressures. However good the drain it still faces a losing battle, but this is also an ultimate limit as the drain is responsible for the maximum possible amount of pore fluid. It is the opposite extreme to the finite unit cell, an “infinite cell”.

Brennan & Madabhushi (2001) examined the theoretical behaviour of a drain in an infinite cell, and identified a boundary representing the extent to which pore fluid uses the drain at a given instant. This expanded with time as pressure drops were communicated in a “Chinese

whisper” between soil elements. The boundary was termed the flow front, representing the boundary between near- and far-field soil, and the limit of horizontal flow. It is suggested that this may be used as a measure of drain performance.

A centrifuge test, AJB-1, was performed on a uniform deposit containing a single coarse-sand drain. Following a model earthquake, excess pore pressures were plotted against horizontal distance in a single plane, here chosen to be a layer at 4m depth. Three times are examined, immediately after the earthquake, then 100s and 200s after the end of the earthquake. This enables flow front propagation to be seen, as shown in Fig.17.

Excess pore pressure has been normalised with initial vertical effective stress σ_{v0}' to form an r_u value, which equals unity at complete liquefaction. Fig.1a clearly demonstrates a zone of slightly reduced pore pressure around the drain, extending to a radius of 1.5m. Fig. 1c shows that this expands to a radius of up to 5m after 200s. However, by now the entire layer has been dissipating fluid vertically, sufficient to reduce r_u in the plane at the far field to 0.5 without the use of a drain. Fig. 1b shows that the flow front has already passed the furthestmost instrumented position. During this first 100s the fluid motion is predominantly horizontal, and constrained within the flow front. After this, substantial vertical dissipation has begun within the layer, and the flow front has slowed as it expands further. It would be expected that velocity should be inversely proportional to radial distance, by continuity.

Flow fronts were observed to be delayed at points nearer the surface, by upwardly draining fluid from below. It may be important to protect the shallower areas more, in which case it is suggested that the intensity of drainage cover for these areas be increased relative to deeper points. In other words, an interspersation of full and partially penetrating drains could be preferable to putting all drains to full depth.

Fig. 18 shows contours of pore pressure in test AJB-5, a group of 13 triangularly spaced drains similar to that of AJB-1, both immediately after the earthquake and 200s later. Circles represent the locations of drains, and crosses the location of instruments. It is seen that zones of

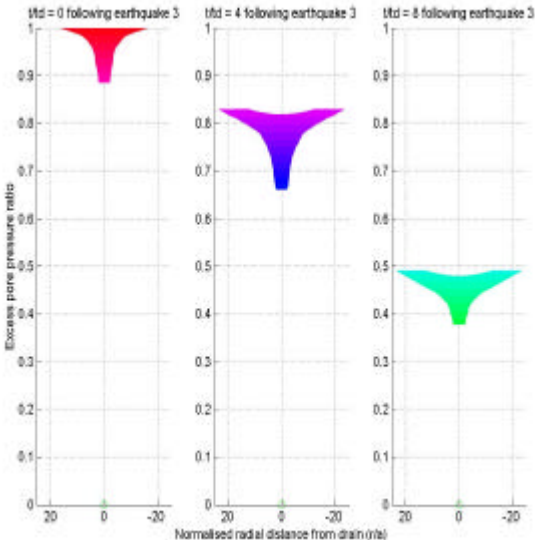


Fig.17 Excess pore pressure ratio measured in centrifuge test AJB-1, versus horizontal distance around a central drain, at a) 0s, b) 200s and c) 400s following the end of shaking.

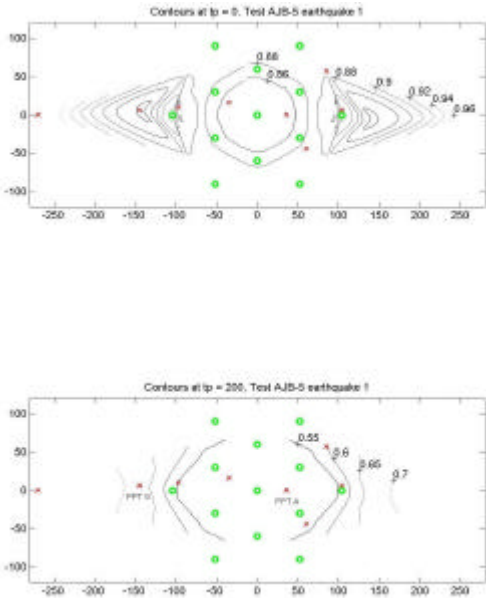


Figure 2. Contours of excess pore pressure measured in centrifuge test AJB-5, in plan view.

reduced pore pressure develop faster and

further within the group than outside.

The internal drains are unhampered by fluid coming from far-off locations. However, the reduced performance of the outermost drains which do have to cope with this has a knock-on effect to their neighbours, who will have more fluid to shift than if all drains had operated in unit cells.

It may be concluded that drain behaviour may be categorised by flow fronts, whose velocity has a bearing on the amount of soil that is remediated. Drainage from depth may have caused delay to surface drainage. In addition, by reconsidering the unit cell assumption when dealing with small drain groups, the spatial extent of treatment may be estimated based on whether any given drain is connected to an infinite fluid source or not, rather than the empirical method of treating an additional lateral region that extends a distance equal to the depth of liquefiable material.

8 Conclusions

At Cambridge University dynamic centrifuge modelling has a long established history of about 25 years. During this period a vast variety of boundary value problems were studied that contributed to the understanding of liquefaction phenomena. Recent developments have taken place to improve earthquake actuation in the form a Stored Angular Momentum (SAM) earthquake actuator. This actuator is able to produce strong earthquakes on models subjected to high gravities. Recent installation of a pneumatic actuator to centralise the mechanism before each earthquake has resulted in reproducible and uniform model earthquakes. Also large model containers that simulate deep sand layers have been developed. Model earthquakes with different magnitudes, variable durations and at different frequency tone bursts or swept sine wave type input motions can be generated using the SAM earthquake actuator.

It is important to understand and quantify boundary effects in soil models being tested on centrifuges. Specialist model containers are currently in use to contain soil models in the centrifuge. Equivalent Shear Beam (ESB) model containers that simulate the dynamic soil stiffness have been developed to minimise boundary effects. At Cambridge an effort is underway to characterise soil models before and after earthquake loading using miniature, in-flight cone penetrometers. Results from these CPT tests have confirmed the uniformity of soil models while helping to quantify the boundary effects close to the end walls of the ESB container.

The developments in dynamic centrifuge modelling outlined here have helped us to study a wide variety of problems such as liquefaction induced lateral spreading, soil flow past piles and the performance of drains to mitigate liquefaction effects. The results from the centrifuge tests can lead not only to a fundamental understanding of the soil behaviour but can help clarify the current design methods or procedures. Centrifuge model testing of shallow saturated slopes with seepage flow parallel to the slope revealed that during earthquake loading the soil suffers contractile and dilative strains during each half of the loading cycle. Similarly, tests on pile foundations in laterally spreading soils reveal that large transient forces may be acting on the pile during part of the loading cycle when suctions are being generated in the soil. This observation has implications in estimating the peak lateral force acting on pile foundations located in laterally spreading soils. Centrifuge model testing of drains in liquefiable soils can help to establish the effectiveness of the drains as liquefaction

mitigation measures. The results from these tests indicate that drain capacity may be an important parameter for effective functioning of these drains in relieving the excess pore water pressures in the ground following liquefaction.

References

- [1] Abdoun, T.H. (1997) "Modelling of seismically induced lateral spreading of multi-layered soil and its effect on pile foundations", PhD Thesis, Rensselaer Polytechnic Institute, NY.
- [2] Boulanger, R.W., Idriss, I.M., Stewart, D.P., Hashash, Y. & Schmidt, B. 1998. Drainage capacity of stone columns or gravel drains for mitigating liquefaction. In ASCE Geotechnical Special Publication no. 75: 678-690.
- [3] Brennan, A.J. & Madabhushi, S.P.G. (2001). Effectiveness of vertical drains in mitigation of liquefaction. 10th International Conference on Soil Dynamics and Earthquake Engineering, Philadelphia, PA.
- [4] Brennan, A.J. & Madabhushi, S.P.G. (2002). Design and performance of a new deep model container for dynamic centrifuge testing. In: Proceedings of the International Conference on Physical Modelling in Geotechnics, St John's, Newfoundland, to be published.
- [5] Brennan, A.J. & Madabhushi, S.P.G. (2002). Liquefaction remediation by vertical drain groups. In, Proceedings of the International Conference on Physical Modelling in Geotechnics (to be published).
- [6] Hamada, M. (1992) "Case studies of liquefaction and lifeline performance during past earthquakes", Technical Report NCEER-92-0001, National Centre for Earthquake Engineering Research, Buffalo, NY. Vol.1 Sec.3.
- [7] Japan Road Association (1996) "Specifications for highway bridges, part V: Seismic design", pp. 90-95, Japan
- [8] Luong, M.P. & Sidaner, J.F. (1981) Undrained Behaviour of Cohesionless Soils Under Cyclic and Transient Loading. Proc. Int. Conf. Recent Advances in Geotechnical Earthquake Engineering and Soil Dynamics, pp.215-220
- [9] Madabhushi, S.P.G., A.N. Schofield and X. Zeng, (1995), Complementary shear stresses in dynamic centrifuge modelling, Dynamic geotechnical testing II, ASTM STP 1213, USA, pp.346-359.
- [10] Madabhushi, S.P.G., Schofield, A.N. and Lesley, S., (1998), A new Stored Angular Momentum (SAM) based Earthquake Actuator, Proc. Cenrifuge'98, Intl. conf on Centrifuge Modelling, Tokyo, Japan.
- [11] Madabhushi, S.P.G., S.K. Haigh and D. Patel, (2001), Geotechnical aspects of the Bhuj earthquake of 26th January 2001, EEFIT Report, Institution of Structural Engineers, London.
- [12] Meyersohn, W.D. (1994) "Pile response to liquefaction-induced lateral spread", PhD Thesis, Cornell University.
- [13] Mitchell, J.K., Baxter, C.D.P. & Munson, T.C. 1995. Performance of improved ground during earthquakes. In ASCE Geotechnical Special Publication no. 49: 1-36.
- [14] National Research Council (1985), "Liquefaction of soils during earthquakes", Report No. CETS-EE-001, Committee on Earthquake Engineering. National Academy Press, Washington, DC.
- [15] Seed, H.B. & Booker, J.R. 1977. Stabilisation of potentially liquefiable sand deposits. ASCE Journal Geotech. Eng. Division. 103(7):757-768.
- [16] Steedman, R.S. (1999). Developments in centrifuge modelling for earthquake geotechnical engineering. In, Seco e Pinto (ed.), Earthquake Geotechnical Engineering: 21-27. Balkema, Rotterdam
- [17] Teymur B. and Madabhushi S.P.G., (2001), CPT assessment of boundary effects in dynamic centrifuge modelling 4th International Conference on Recent Advances in Geotechnical Earthquake Engineering and Soil Dynamics, San Diego, March.
- [18] Zeng, X. and A.N. Schofield, (1996), Design and performance of an equivalent-shear-beam container for earthquake centrifuge modelling, Geotechnique, Vol.46, No.1, pp. 83-102.